Ferromagnetic domain distribution in thin films during magnetization reversal

W.-T. Lee,[1] S. G. E. te Velthuis,[2] G. P. Felcher,[2] F. Klose,[1] T. Gredig,[3] and E. D. Dahlberg[3]
[1]*Spallation Neutron Source, Oak Ridge National Laboratory, Oak Ridge, Tennessee 37831*
[2]*Materials Science Division, Argonne National Laboratory, Argonne, Illinois 60439*
[3]*Department of Physics, University of Minnesota, Minneapolis, Minnesota 55455*
(Received 20 December 2001; revised manuscript received 8 April 2002; published 3 June 2002)

It is shown that polarized neutron reflectometry can determine in a model-free way not only the mean magnetization of a ferromagnetic thin film at any point of a hysteresis cycle, but also the mean-square dispersion of the magnetization vectors of its lateral domains. This technique is applied to elucidate the mechanism of magnetization reversal of an exchange-biased Co/CoO bilayer. The reversal process above the blocking temperature T_b is governed by uniaxial domain switching, while below T_b the reversal of magnetization for the trained sample takes place with substantial domain rotation.

DOI: 10.1103/PhysRevB.65.224417 PACS number(s): 75.25.+z, 75.60.Jk, 75.70.−i

Polarized neutron reflectometry (PNR) was introduced in the beginning of the 1980s to map the magnetic profiles of thin films and multilayers.[1–3] This technique has been applied to study systems in which the magnetic structure consists of a stack of laterally uniform magnetic layers. The experiments reveal the depth dependence of the magnetization, in size as well as in direction: this is the information needed to characterize magnetic interactions between different layers. Polarized neutron reflectometry can also be instrumental in understanding a different, but still outstanding problem in magnetism: the breakdown into domains of a ferromagnet during the hysteresis cycle.[4] While neutron reflectivity studies are limited to samples in the form of thin flat films, this is the form of many magnetic systems created in recent years for diverse applications, from magnetic recording to magnetic memory to sensors. Magnetic domains significantly impact the performance of these devices. In most applications the ferromagnetic layers are so thin that only a single magnetic domain can be energetically stable through the thickness. While passing through a hysteresis loop, however, the film may break down into a collection of magnetic domains within the film plane (i.e., *lateral* domains), each characterized by a size and a direction of magnetization. In spite of the progress made in the use of microscopic and scattering probes, the problem of observing these domains—especially at some distance below the surface—remains difficult. Yet, as demonstrated in this paper, a statistical measure of the domain distribution can be obtained directly from PNR.

In a PNR experiment, the intensity of the neutrons reflected from a surface is measured as a function of the component of the momentum transfer that is perpendicular to the surface, $q_z = 4\pi \sin\theta/\lambda$, where θ is the angle of incidence (and reflection) and λ the neutron wavelength. Since q_z is a variable conjugate of the depth z from the surface of the film, a scan over a suitable range of q_z provides excellent information on the chemical and magnetic depth profile of the film. When the incident neutrons are polarized along an applied magnetic field **H**, and the polarization after reflection is analyzed along the same axis, four reflectivities are recorded: R^{++}, R^{+-}, R^{-+}, R^{--}. The first (second) sign refers to the incident (reflected) neutron polarization with respect to **H**.

Conventionally, a fitting procedure allows a model magnetic profile to be obtained from the spin-dependent reflectivities. However, simple and transparent relations are available, linking the magnetization to the reflectivities. When the direction of magnetization **M** and the applied field are in the film's plane, and **M** is at an angle φ with **H**, then,[5]

$$\frac{R^{++}(\varphi)-R^{--}(\varphi)}{R_s^{++}(0°)-R_s^{--}(0°)} = \frac{R^{+}(\varphi)-R^{-}(\varphi)}{R_s^{+}(0°)-R_s^{-}(0°)} = \cos\varphi, \quad (1)$$

$$\frac{R^{-+}(\varphi)}{R_s^{-+}(90°)} = \sin^2\varphi. \quad (2)$$

These relations are valid at all values of q_z above the critical edge for total reflection, provided that the direction of **M** is constant along the thickness of the film. The normalizing quantities $R_s(0°)$ and $R_s(90°)$ refer to reflectivities measured with **M** aligned parallel and perpendicular to the neutron polarization, respectively. The single-superscript reflectivities are those measured without polarization analysis, i.e., $R^{+} = R^{++} + R^{+-}$ and $R^{-} = R^{--} + R^{-+}$ (for this configuration of fields, $R^{+-} = R^{-+}$).

When a film breaks down into lateral domains, the effect on the reflectivity will depend on the size of the domains. Infinitely large domains specularly reflect plane waves. For finite domains the reflected beam has some divergence, which is inversely proportional to the domain size. Since the incident beam itself has some divergence, for each instrument there is a minimum size of the domains for which there is a recognizable broadening. For domains larger than this length, the intensities reflected from different domains superimpose incoherently in the specular beam. In this case, the terms in φ of Eqs. (1) and (2) can now be interpreted as averages across the sample plane. While the term $\langle\cos\varphi\rangle$ may be measured as well by conventional magnetometery, $\langle\sin^2\varphi\rangle$ provides information leading to the mean-square dispersion of the domain orientations χ^2:

$$\chi^2 = \langle\cos^2\varphi\rangle - \langle\cos\varphi\rangle^2 = \left\{1 - \frac{R^{-+}(\varphi)}{R_s^{-+}(90°)}\right\} - \left\{\frac{R^{++}(\varphi)-R^{--}(\varphi)}{R_s^{++}(0°)-R_s^{--}(0°)}\right\}^2. \quad (3)$$

 ©2002 The American Physical Society

These quantities are constant, and independent of q_z, if the domains extend through the entire thickness of the film. As a comparison with (transverse) magneto-optic Kerr effect (MOKE), one can measure $\langle \cos\varphi \rangle$ and $\langle \sin\varphi \rangle$, but not $\langle \sin^2\varphi \rangle$.

Recapitulating the universality of the method, it can be stated that PNR can be applied to measure the mean magnetization and the mean-square dispersion of domains on thin films, provided that the following hold.

(1) The film is flat and smooth enough to reflect neutrons.
(2) The reflectivity with neutrons polarized perpendicularly to the film's magnetization in the saturated state can be obtained. In the case in which a direct measurement is not possible, the reflectivity curve can, in principle, be calculated from a model of the saturated film that has been derived through other means, for instance, reflectivity measurement with the film saturated parallel to the neutron polarization.

The two quantities **M** and χ^2 that have been extracted from the data are valid provided that:

(1) $\langle \cos\varphi \rangle$ and $\langle \sin^2\varphi \rangle$ are independent of q_z.
(2) The reflected beam is not appreciably broader than the incident beam.

Although a robust analysis of the limits of validity has not been devised yet, some rules of thumb are provided below for a practical example.

These ideas have been applied in the study of the magnetic behavior of a partially oxidized Co film[6,7] that exhibits exchange bias.[8] A nominal 120-Å-thick polycrystalline Co film was deposited on a silicon substrate by magnetron sputtering. Its surface was then oxidized in ambient atmosphere to form an ≈30-Å-thick CoO top layer. Since the Co layer was thinner than a domain wall (~500 Å),[4] only one domain was expected along the sample's thickness. At the same time, the shape anisotropy constrained the magnetization to be in the plane of the film. The neutron measurements were carried out at the POSY I reflectometer at the Intense Pulsed Neutron Source of Argonne National Laboratory. POSY I is a time-of-flight reflectometer, utilizing neutron wavelengths comprised between 2 and 14 Å.[9] It is equipped with an analyzer consisting of a polarization splitter.[10] For the evaluation of $\langle \sin^2\varphi \rangle$ in relation (2), we use R^{-+} from measurements with the analyzer. For the evaluation of $\langle \cos\varphi \rangle$ in relation (1), we use R^+ and R^- measured without the analyzer. Figure 1 shows the R^+ and R^- reflectivity pattern of the film at saturation. The reflectivity was taken at 10 K. The fitted profile of the scattering amplitude densities gives the thickness of the layers, the interface roughness between the ferromagnetic (FM) Co and the antiferromagnetic (AF) CoO layers, and the ferromagnetic contribution from Co. The AF order of CoO is not considered in the analysis, because for this range of q_z the scattering properties are averaged over a length scale that well exceeds the antiferromagnetic period of CoO.

Films of this type have been found to have three magnetic phases. At temperatures higher than the Néel temperature T_N, the magnetization follows a square hysteresis loop. As the temperature is lowered, the hysteresis loop becomes *S* shaped and exhibits a scaling behavior as a function of the coercive field and a characteristic temperature below T_N.[11] If the sample is field cooled to below the "blocking temperature" T_b,[12] exchange bias appears—the hysteresis loop is no longer symmetric with respect to the applied field. Figure 2 shows the hysteresis loops of our film above and below $T_b \sim 130$ K, at 140 and 10 K, respectively, after field cooling in +5 kOe from room temperature. The cooling and measurement fields were along the same axis, parallel to an arbitrary direction in the film surface. At 140 K, the hysteresis loop is symmetric with a coercive field $H_C = 100$ Oe. At 10 K, the initial reversal after field cooling ($A2 \rightarrow B2$) has a sharply squared shape and a large reversal field ($H_a = -1.1$ kOe). Subsequent loops (through $C2$, $D2$, etc.) exhibit a more gradual *S* shape, with $H_a = +300$ Oe at one side and H_a

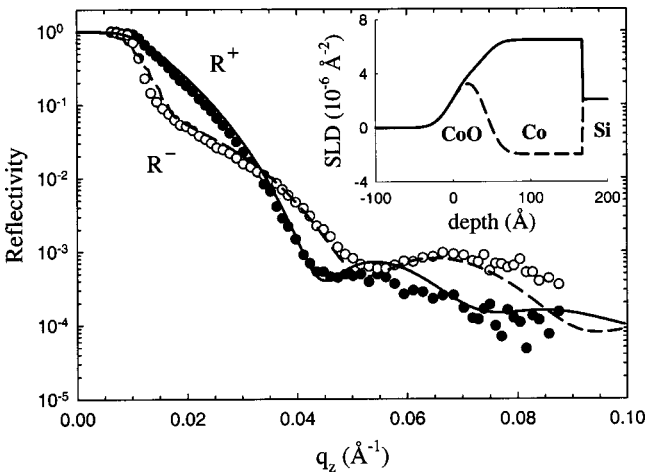

FIG. 1. Polarized neutron reflectivity of a Co/CoO bilayer on Si in a saturating field of 5 kOe. Both measured points and calculated lines are presented for incident neutrons polarized parallel (R^+) and antiparallel (R^-) to the applied field. The inset shows the scattering length density profile calculated for the two spin states. The layer thickness for Co and CoO were found to be 130 and 45 Å, respectively, with a half-width roughness of 15 Å between the two and 15 Å at the film surface.

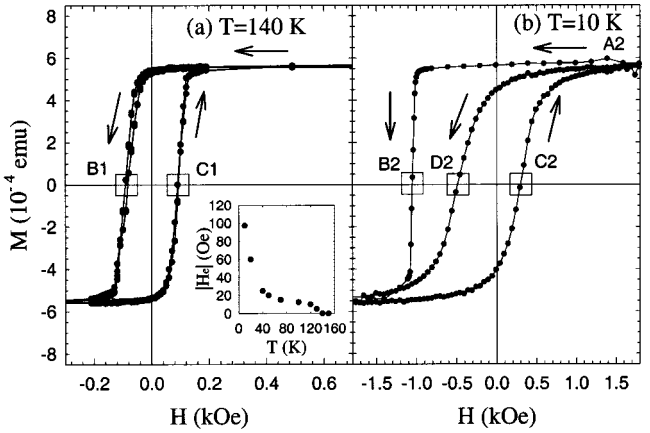

FIG. 2. Hysteresis curves (a) above T_b at 140 K and (b) below T_b at 10 K. The labels ($A2$ at M = saturation, others at $M = 0$) indicate locations where neutron reflectivities are measured. The inset shows the temperature dependence of the bias field $|H(T)|$.

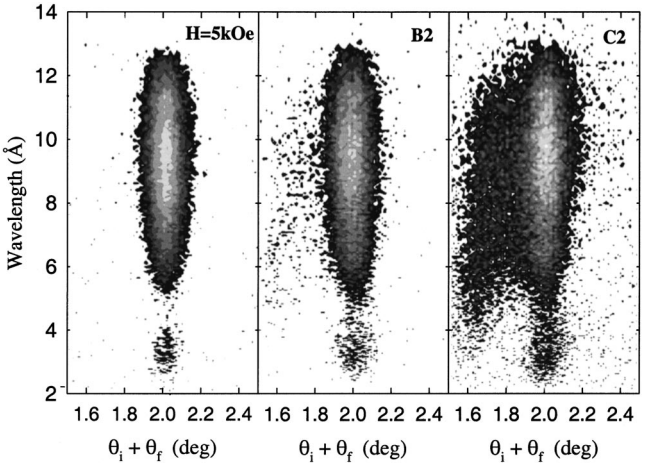

FIG. 3. Contour plots of the specularly reflected beam (+ state) at $T=10$ K, at saturation, the reversal point $B2$ of the untrained film, and the reversal point $C2$ of the trained film. The reflected beam is reflected, at all wavelengths, at an angle θ_f equal to the angle of incidence. While the specular peak width has not increased significantly, Yoneda scattering emerges in $B2$ and $C2$.

$=-500$ Oe at the other side, giving a bias field $H_e=-100$ Oe. The inset of Fig. 2 shows the temperature dependence of the bias field of the trained sample, for which $T_b \sim 130$ K.

To elucidate the mechanism of reversal of the magnetization, PNR measurements were taken close to the reversal points where $M=0$, as marked in Fig. 2, as well as at saturation. The width of the reflection lines in all cases was not appreciably broader than expected on the basis of the instrumental resolution, as it can be seen in Fig. 3. The instrumental width of the reflection line is such to make difficult the evaluation of domain sizes exceeding 20 μm. In addition to the specular beam, a faint off-specular scattering, of the Yoneda type,[13] was found when the sample was not in a saturated state.[7] While the details of this scattering are the subject of a separate investigation, its size is such, never exceeding a few percent of the reflected beam, that neglecting it does not affect the conclusions reached here.

The spin-flip reflectivities R^{-+} (before correcting for instrument efficiency) are presented in Fig. 4. They are obtained from measurements at both the ascending and descending reversal points. The spin-flip reflectivity measured at saturation $R_s^{-+}(0°)$ (ideally equal to 0) is indicative of the polarizing efficiency of polarizer and analyzer. In order to obtain the normalizing reflectivity $R_s^{-+}(90°)$, the sample was field cooled in $H=2000$ Oe to 10 K. Then the field was brought to zero (a guide field of a few oerateds in a perpendicular direction was sufficient to orient the neutron spins, but too weak to affect the magnetization). The procedure was made possible because for this sample the remnant magnetization after field cooling is close to the saturated value. $R_s^{-+}(90°)$ obtained was used to normalize the measurements at the reversal points at both temperatures, as the reflectivities from a saturated film as such do not change between 10 and 140 K. The reflectivities R^+ and R^- measured at the reversal points are presented in Fig. 5. It was trivial to obtain

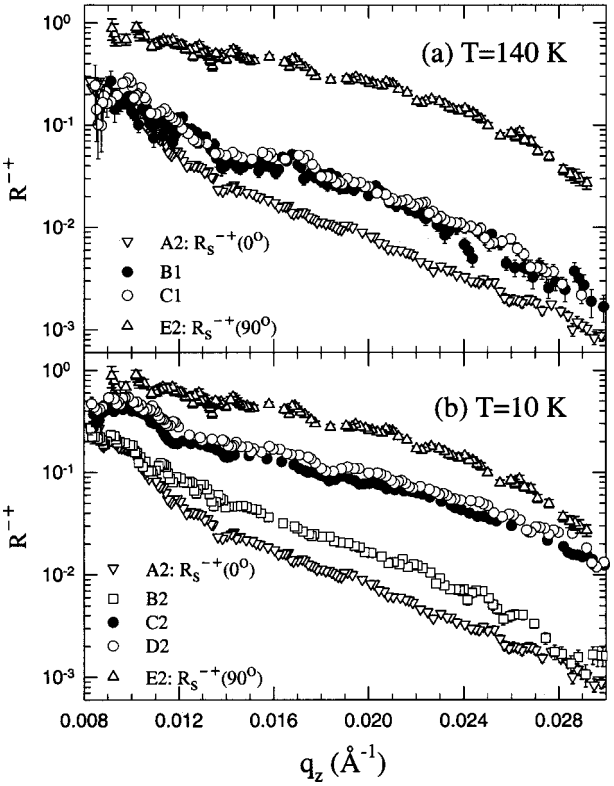

FIG. 4. The spin-flip reflectivities R^{-+} (a) at 140 K, at the reversal points ($B1$ and $C1$); (b) at 10 K, at reversal points of the untrained film ($B2$) and the trained film ($C2$ and $D2$), compared to those measured with the magnetization saturated along the field $R_s^{-+}(0°)$ ($A2$) and perpendicular to the field $R_s^{-+}(90°)$ ($E2$).

the reflectivities at saturation, $R_s^+(0°)$ and $R_s^-(0°)$, with the neutron quantization axis parallel to the magnetization. To within measurement error, R^+ and R^- at the reversal points are identical, giving $\langle \cos\varphi \rangle \sim 0$ over the entire q range. The q_z dependence of χ^2 (Fig. 6) was obtained by processing the spin-flip intensities R^{-+} according to Eq. (3) and correcting for the efficiencies of the instrument.

The spin-flip reflectivity (Fig. 4) and consequently χ^2 (Fig. 6) is very dependent on temperature and training. To put in perspective the results, let us consider the extreme cases (Fig. 7) for $M=0$ ($\langle \cos\varphi \rangle = 0$). $\chi^2=0$ means that $\langle \sin^2\varphi \rangle = 1$, so all the moments are oriented perpendicular to **H**, implying that the reversal occurs through magnetic domain rotation. In contrast $\chi^2=1$ means $\langle \sin^2\varphi \rangle = 0$ so that half of the moments are parallel and half antiparallel to the field: the reversal occurs by uniaxial domain switching. For an isotropic distribution of the domains, $\chi^2=0.5$. While a χ^2 value between 0 and 1 does not uniquely identify a particular distribution, it indicates an angular spread of the domains. As seen in Fig. 6(a), χ^2 measured at the reversal points at 140 K ($B1$ and $C1$) deviates only slightly from unity: above T_b, the magnetization reversal occurs primarily through uniaxial domain switching. Similarly, in Fig. 6(b) reversal of the untrained film at 10 K ($B2$) gives χ^2 close to unity. In contrast, the χ^2 values are much smaller for the trained film at the two reversal points $C2$ and $D2$. The pertinent χ^2 values, ranging

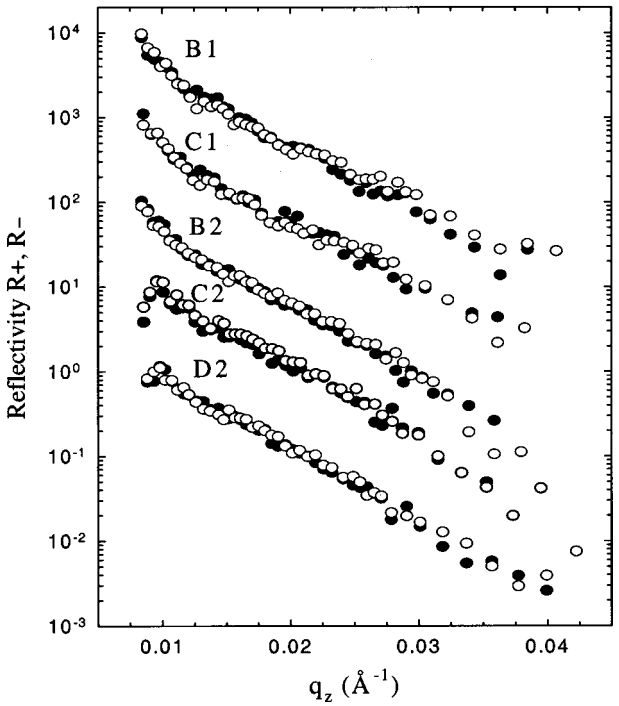

FIG. 5. Reflectivities R^+ and R^- at 140 K, at the reversal points ($B1$ and $C1$); and at 10 K, at reversal points of the untrained film ($B2$) and the trained film ($C2$ and $D2$). The reflectivities are displaced by factors of 10 for clarity.

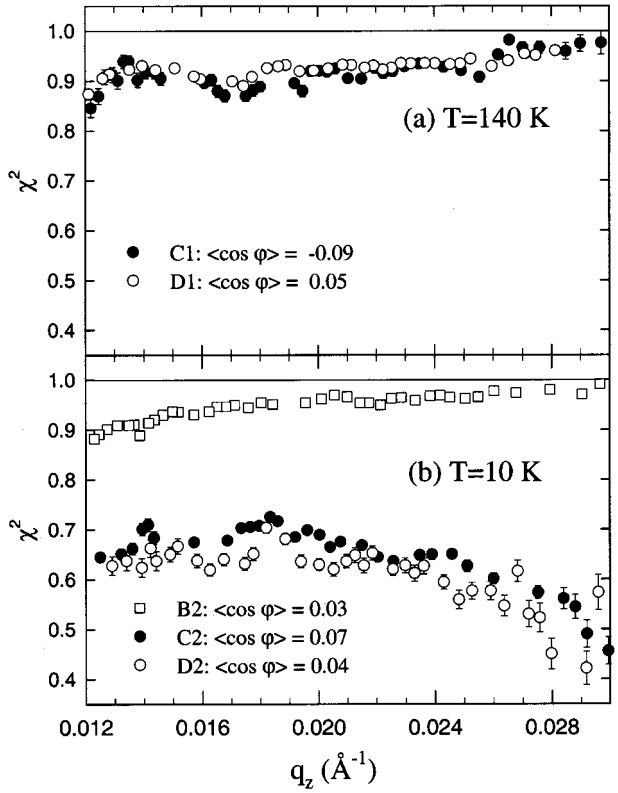

FIG. 6. Mean-square dispersion of lateral domain orientation χ^2 (a) at 140 K, at the reversal points ($B1$ and $C1$); (b) at 10 K, at reversal points of the untrained film ($B2$) and the trained film ($C2$ and $D2$).

from 0.50 to 0.65, indicate a breakdown in domains with a substantial angular spread of their magnetic orientations.

The present results substantiate a model recently proposed[11] for the magnetic behavior of Co/CoO. Above the blocking temperature, the *S*-shaped hysteresis loop has been interpreted in terms of a modified Ising model. The FM Co layer is comprised of a number of domains for which the applied field determines the direction of the magnetization.[14] Their reversal takes place over a finite interval of fields because of a range of coupling strengths with different antiferromagnetic CoO domains.[15] The orientation of the sublattice magnetization of the AF domains is not fully locked by the crystalline anisotropy and the coupling between different AF domains. Below T_b, however, the AF domains are stabilized. The orientation of the sublattice magnetization of CoO now strongly influences the direction of the FM domains. Unless a strong external magnetic field is present, the FM domains turn their magnetization in the direction optimizing both the coupling with the AF domains and the Zeeman energy,[16,17] giving rise to the rotation of domains we observed.

The results obtained for $T<T_b$ may be compared with those obtained on a different exchange-bias system: ferromagnetic Fe coupled with antiferromagnetic FeF_2.[18] The type of neutron measurements carried out in the two cases is similar: the four spin-dependent reflectivities have been measured close to the $M=0$ points of the hysteresis loop. The results reflect the inherent difference of the two physical systems. In the polycrystalline Co/CoO bilayer, a fairly isotropic ferromagnetic domain distribution of Co implies that the AF domain distribution of CoO is equally isotropic. In FeF_2 grown semiepitaxially on MgO(100), AF domains are formed with their sublattice magnetization rigidly aligned along two perpendicular axes. Consequently the orientation of the ferromagnetic domains of polycrystalline Fe, grown on the top of FeF_2, had to be more constrained at the $M=0$ points of the hysteresis loop, as it was confirmed by comparing the experimental reflectivities with those calculated for a model structure with appropriate distributions of domains.

We have shown that a model-free analysis of reflectivity measurements on a thin film composed of a collage of mag-

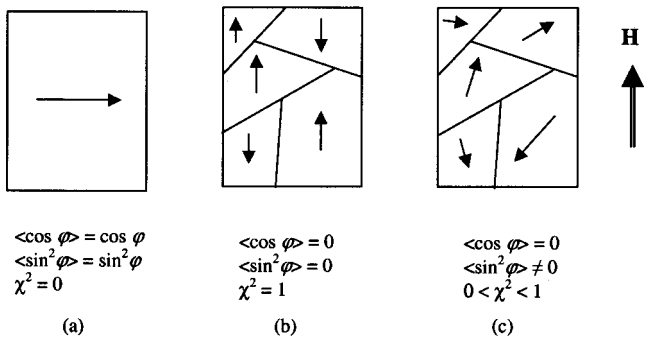

FIG. 7. Schematic diagrams illustrating some possible magnetic configurations in the thin film and the corresponding values of $\langle \sin^2 \varphi \rangle$ and χ^2 (all have $\langle \cos \varphi \rangle = 0$): (a) single domain, (b) collinear domains with magnetization along the applied field H, (c) domains with a dispersion of magnetic orientations.

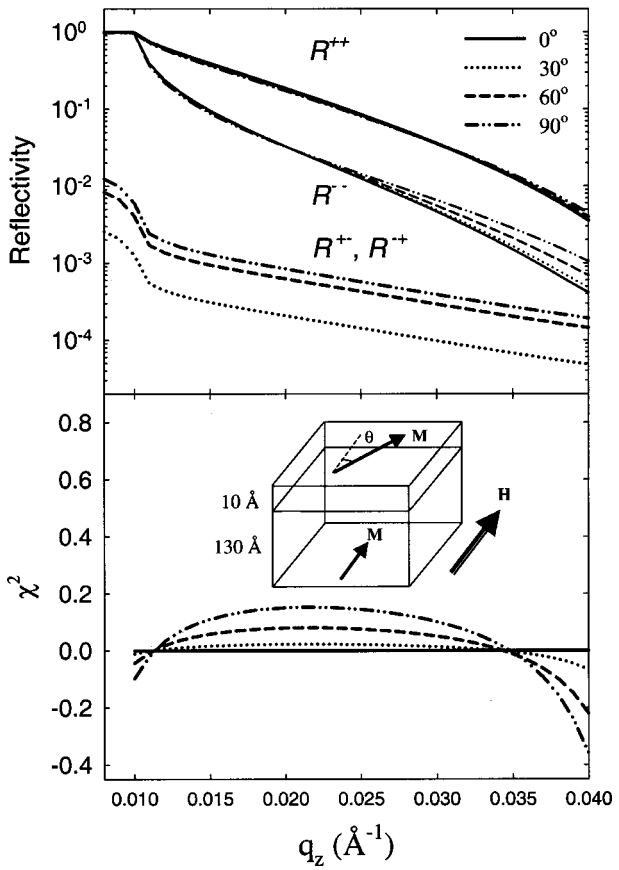

FIG. 8. Reflectivity calculated for a 140-Å thin film of Co (on silicon) of which the surface layer (10 Å) is magnetized at an angle with the applied field. The bottom picture shows how the misalignment of magnetization of a small region may affect the determination of χ^2. The crossing point of the envelope of calculated χ^2 is at $q=0.035$ Å^{-1}, at a value $2\pi/d$ given by approximately (i.e., in the first Born approximation) the thickness d of the magnetic layer.

netic domains provides not only the average magnetization, but also the mean-square dispersion of the domain orientations. Applying this analysis to the $M=0$ points of the hysteresis cycle in an exchange-biased Co/CoO sample revealed that the reversal mechanisms are different above and below the blocking temperature. The applicability of this method partly relies on the possibility to obtain the normalizing quantity appearing in Eq. (2), $R_s^{-+}(90°)$. Furthermore, with respect to the domain size issues, it may be possible to apply the method for small domains, provided that all neutrons scattered in a broader reflectivity line are properly counted and correlation effects between the magnetization of adjacent domains are taken into account.[19] The weak, but nonzero dependence of χ^2 on q_z that is observed for Co/CoO could indicate that the direction of magnetization is not completely uniform throughout the thickness. The simulations shown in Fig. 8 give a measure of the sensitivity of reflectivity to a magnetic structure in which the direction of magnetization is depth dependent. Although a general theoretical basis for interpreting all reflectivity patterns is not available yet, the experiment itself seems to offer a number of checks on the validity of the procedure.

If used as described above, PNR does not need detail structural modeling to obtain $\langle \cos\varphi \rangle$ and χ^2 at any point of a hysteresis cycle. Technically it is becoming feasible to measure a reflectivity curve in a matter of minutes, a data-acquisition rate comparable to that of conventional magnetization measurements. Both $\langle \cos\varphi \rangle$ and χ^2 measured by PNR can then be compared with the results of micromagnetic calculations.[20] Even more desirable is the development of a theoretical framework along the lines of the work done to extract information from the magnetization—as obtained by passing with minor hysteresis loops through different paths of metastable states.[21,22] If not only the average magnetization but also χ^2, the mean-square dispersion of the domain orientations, is available, how much easier or more realistic becomes the analysis of the magnetization process?

Work done at the Argonne National Laboratory was supported by U.S. DOE, Office of Science Contract No. W-31-109-ENG-38 and by Oak Ridge National Laboratory, managed for the U.S. DOE by UT-Battelle, LLC under Contract No. DE-AC05-00OR22725. Work done at the University of Minnesota was supported by the NSF MRSEC NSF/DMR-9809364.

[1] J. F. Ankner and G. P. Felcher, J. Magn. Magn. Mater. **200**, 741 (1999).
[2] C. F. Majkrzak, Physica B **221**, 342 (1996).
[3] H. Zabel, R. Siebrecht, and A. Schreyer, Physica B **276**, 17 (2000).
[4] *Magnetic Domains: The Analysis of Magnetic Microstructures*, edited by A. Hubert and R. Schäfer (Springer-Verlag, Berlin, 1998); G. Bertotti, *Hysteresis in Magnetism* (Academic, New York, 1998).
[5] N. K. Pleshanov, Physica B **269**, 79 (1999).
[6] B. H. Miller and E. D. Dahlberg, Appl. Phys. Lett. **69**, 3932 (1996).
[7] S. G. E. te Velthuis, A. Berger, G. P. Felcher, B. K. Hill, and E. D. Dahlberg, J. Appl. Phys. **87**, 5046 (2000).
[8] W. H. Meiklejohn and C. P. Bean, Phys. Rev. **105**, 904 (1957); J. Nogués and L. Schuller, J. Magn. Magn. Mater. **192**, 203 (1999); A. E. Berkowitz and K. Takano, *ibid.* **200**, 552 (1999).
[9] G. P. Felcher, R. O. Hilleke, R. K. Crawford, J. Haumann, R. Kleb, and G. Ostrowski, Rev. Sci. Instrum. **58**, 609 (1987).
[10] Th. Krist, F. Klose, and G. P. Felcher, Physica B **248**, 372 (1998).
[11] A. Berger, A. Inomata, J. S. Jiang, J. E. Pearson, and S. D. Bader, Phys. Rev. Lett. **85**, 4176 (2000).
[12] P. J. van der Zaag, Y. Ijiri, J. A. Borchers, L. F. Feiner, R. M. Wolf, J. M. Gaines, R. W. Erwin, and M. A. Verheijen, Phys. Rev. Lett. **84**, 6102 (2000).
[13] Y. Yoneda, Phys. Rev. **131**, 2010 (1963).
[14] M. D. Stiles and R. D. McMichael, Phys. Rev. B **63**, 064405 (2001).

[15] F. Nolting, A. Scholl, J. Stöhr, J. W. Seo, J. Fompeyrine, H. Siegwart, J.-P. Locquet, S. Anders, J. Lüning, E. E. Fullerton, M. F. Toney, M. R. Scheinfein, and H. A. Padmore, Nature (London) **405**, 767 (2000).

[16] T. Gredig, I. N. Krivorotov, C. Merton, A. M. Goldman, and E. D. Dahlberg, J. Appl. Phys. **87**, 6418 (2000).

[17] V. Ström, B. J. Jönsson, K. V. Rao, and E. D. Dahlberg, J. Appl. Phys. **81**, 5003 (1997).

[18] M. R. Fitzsimmons and P. Yashar, C. Leighton, I. K. Schuller, J. Nogués, C. F. Majkrzak, and J. A. Dura, Phys. Rev. Lett. **84**, 3986 (2000).

[19] B. Toperverg, O. Nikonov, V. Lauter-Pasyuk, and H. J. Lauter, Physica B **297**, 169 (2001).

[20] H. Kronmüller and R. Hertel, J. Magn. Magn. Mater. **215**, 11 (2000).

[21] E. C. Stoner and E. P. Wohlfarth, Philos. Trans. R. Soc. London, Ser. A **240**, 599 (1948).

[22] F. Preisach, Z. Phys. **94**, 277 (1935); I. D. Mayergoyz, *Mathematical Model of Hysteresis* (Springer-Verlag, New York, 1991).